UBC Social Ecological Economic Development Studies (SEEDS) Sustainability Program

Student Research Report

U-Square Mobile: Phase 3 (Urban Turbine Dashboard)

Curtis Catt, Felipe Solano, Jason Chow, Vincent Hanley, Omar Qazi

University of British Columbia

Course: ELEC 491

Themes: Transportation, Land

Date: April 20, 2020

ELEC 491: Electrical Engineering Capstone Design Project

Design Document

Capstone #92 Urban Turbine: U-Square Mobile Dashboard

Prepared by:

Curtis Catt

Felipe Solano

Jason Chow

Vincent Hanley

Omar Qazi

Client: UBC SEEDS Sustainability Program

April 2020

Contents

List of Tables

List of Figures

1. Introduction

U-Square Mobile is an artistic structure proposed by AMS Sustainability and UBC SEEDS Sustainability Program to showcase alternative energy in an interactive piece for the UBC community. It will be placed in the U-Square plaza between the AMS Student Nest and Robert H. Lee Alumni Centre. This iteration of the Urban Turbine project focuses on the electrical system required for the project. In previous years the mechanical system was completed and this year the client has set the goal of finishing the Urban Turbine project. We have identified the following components for the electrical subsystem:

1. AC generators
2. Battery
3. Charge controller
4. Hand crank circuit
5. Sensors
6. Microcontroller
7. Display dashboard
8. Printed circuit board
9. Firmware Design

Design Overview

The structure consists of a main 12-ft steel structure, designed by Michael Kingsmill, on which the wind turbine is located. The user interaction element consists of a display board and a hand crank which are housed on the main body of the structure at a height of about 3-ft. The main electrical subsystem designed by this team is described below.

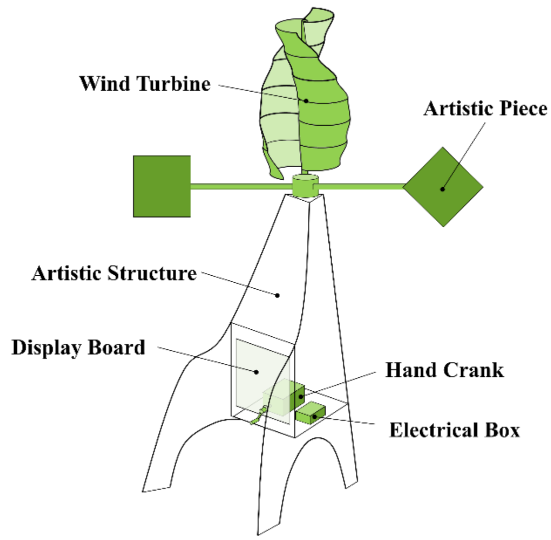

Figure 1 Components of U-Square Urban Turbine

1.1. High Level Design

The final electrical system implemented for power generation consists of a 300W wind turbine which has been previously purchased by the client, a boost MPPT Controller with dump load integration, a 12V battery, and a control circuit. Figure 2 shows the general overview of the electrical system.

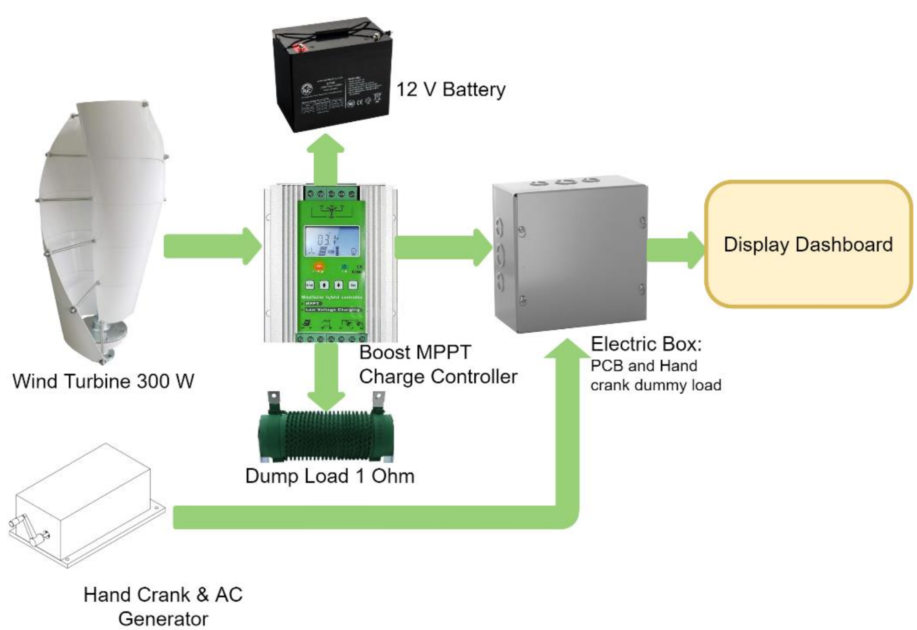

Figure 2 Interconnection of main electrical components

The high-level design shown in demonstrates the layout out of the Urban Turbine's electrical components while showing the system inputs and outputs. The hand crank is connected to a dummy load via the current sensor in series. This means that the hand crank itself is not being used as an energy source for the system. The hand crank is only being used for comparing the power produced by it versus the power produced by the vertical wind turbine.

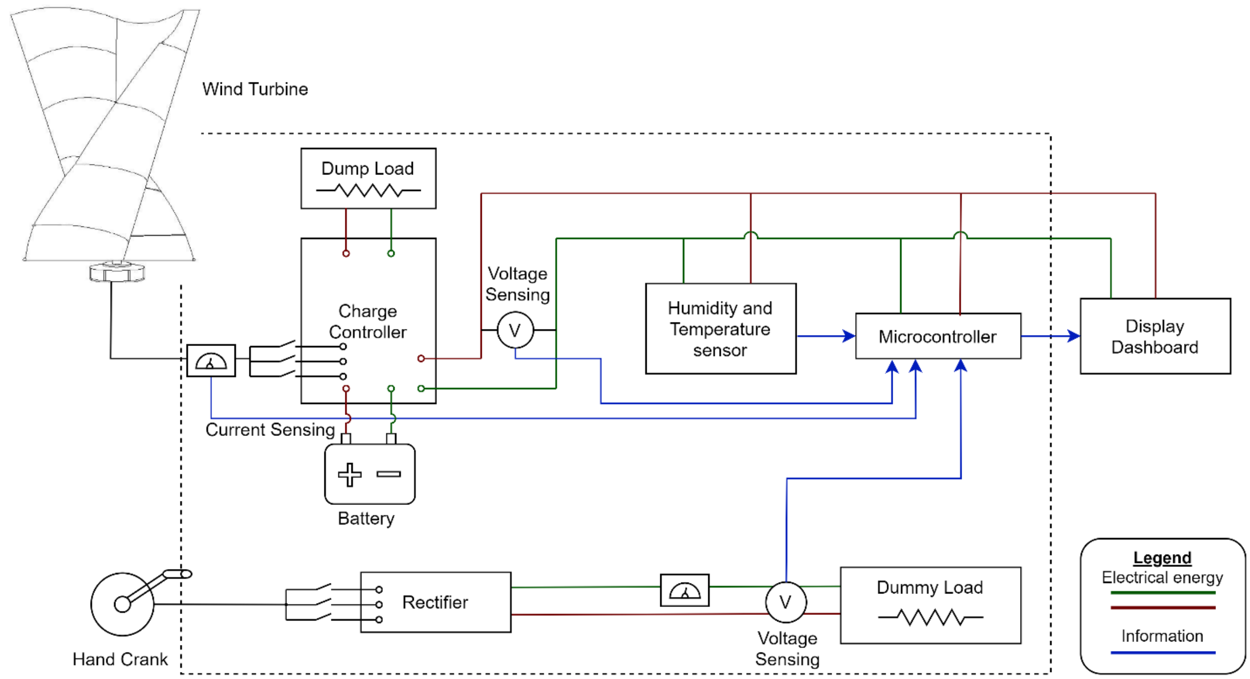

Figure 3 High- level block diagram

2. Components

2.1. AC Generator

Two synchronous generators are included in the design. Despite the budget constraint, the generators had already been chosen by the previous capstone groups, and so we will not choose new generators. Additionally, having two generators greatly simplifies the mechanical engineering work that would be associated with having two inputs (hand crank and turbine) to one generator.

2.2. Battery

In order to choose an appropriate battery, the first task is to calculate the maximum estimated power of the electrical components of the Urban Turbine.

Component(s)	**Estimated Power Draw (mW)**
Microcontroller - ATMEGA328P	<25
Environmental sensor – HIH6300	<5
2* ER-OLEDM024-2G - 128x64 green pixels OLED displays	<600
3* ER-OLEDM024-2W - 128x64 white pixels OLED displays	<900
Charge Controller - JW1230 Boost MPPT Wind Solar Hybrid Charge Controller	<50
20* WS2812B Addressable RGB LEDs	<5000
ACS724 Current sensor	<75
Motion Sensor	<25
Misc. Power Draw (excluding wiring)	<100
Max Power Draw (estimate)	6.8W

Table 1 Maximum estimated power draw

Maximum Estimated Daily Power Consumption $= \ ((Max\ Power\ Draw) * (Hours\ in\ a\ day)) \ = \ (6.905 * (24)) \ = \ 165.72\ Wh$

Provided that all components are operating the power draw of the electrical system is approximately 7 watts. Therefore, this translates into a daily estimated power usage of 165.72 Wh. As a result, a standard was decided after consultation with the client and team members for sizing an appropriate battery. The battery should be able to provide enough energy to power electrical components operating continuously for an entire day while draining the battery at most 50% of its rated capacity. This will provide enough overheard in case of a malfunction that would prevent the display dashboard from shutting down when there is no human presence detected.

Max Estimated Daily Power Consumption = 50% Battery Capacity, thus
New Battery Capacity (Wh) = $2 * 165.72 = 331.44\ Wh$
Battery Size (Ah) = $(Wh)/(Voltage\ rating) = \ (331.44)/12 \ = \ 27.62\ Ah$
Battery Size with Aging Factor (IEEE Std 450-1995) = $(Aging\ Factor) \ * \ (Battery\ Capacity) \ = \ (1.25) * (27.62) \ = \ 34.525\ Ah$

The calculation shows that the battery should be rated for at least 35 Ah. The existing battery i.e. the D75S AGM – VRLA Battery from last year's phase of the project exceeds this requirement as it is rated for 75 Ah. In addition, it also fulfills the following criteria:

1. The battery is a 12V battery which meets the MPPT charge controller's rating.
2. The battery has relatively high endurance i.e. it is able to last up to 500 charging cycles with 50% depth of discharge.
3. Able to operate at least within the temperature range of -15°C to 35°C as Vancouver temperature has varied within that range over the past 10 years[1]
4. Has an average life expectancy of 5 years
5. Able to provide power to the display dashboard for 1 a day with only 50% discharge

2.3. Charge Controller

Due to the complexity of charge controllers, we are using an off-the-shelf product for the charge controller. The charge controller is chosen for the specified output voltage of the battery and for its maximum output current capabilities. The team also explored building a custom controller but that is not completed due to the time constraints for the project.

Option A: FW03-12 Wind Charge Controller

The FW03-12 Wind Charge Controller is a low-cost charge controller rated for 12V generators, with a low (<=240 mW) power draw. The controller performs rectification of the AC output of the wind turbine, and interfaces with a 12V battery to charge it. The charge controller also features an auto-braking function that is activated when the generator produces more than 15V or if the battery is fully charged. One of its main downsides is its lack of boosting capability of the input voltage. This means that the controller is unable to charge the battery at low wind speeds.

[1] Source: https://vancouver.weatherstats.ca/)

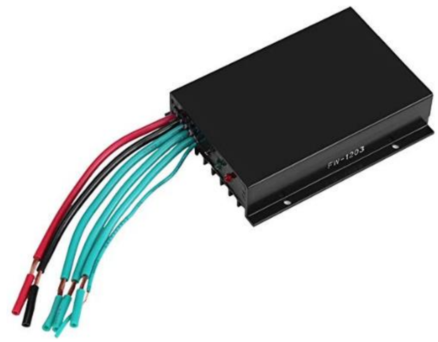

Figure 4 FW-1203 Charge controller

Option B: JW1230 Boost MPPT Wind Solar Hybrid Charge Controller

The JW1230 Boost MPPT Wind Solar Hybrid Charge Controller is a slightly more expensive option rated for a 12V battery. The controller performs rectification of the 3-phase AC output of the wind turbine, and interfaces with a 12V battery to charge it. The benefit of using a boost converter is that, on days with lower wind speeds, the voltage produced by the generator on its own is not high enough to charge the battery; the boost converter increases the voltage produced by the turbine and is then able to charge the battery. The controller allows for user-programmable parameters such as floating voltage, under-voltage, over-voltage, as well as the braking-voltage that will connect the 1Ω 300W resistor to slow the turbine down in high-wind conditions.

Figure 5 JW1230 MPPT Charge Controller and 300W 1Ω resistor.

Although the MPPT charge controller costs $60 more than the low-cost option, we have decided to use it in our design. One of the main reasons being that, while conducting our tests, we found it quite challenging to be able to produce a voltage high enough to charge the battery without the boost. The boost functionality is a necessary feature for the charging at low wind speeds. The customizable input parameters such as battery over-voltage level are useful as it provides more flexibility in being able to configure the controller to the right specifications i.e. 13.8 V for the AGM battery. The LCD screen of the MPPT controller is also an advantage as it provides us with more information that allows us to optimize the charging of the battery.

2.4. Hand Crank

The hand crank adds an interactive piece to the system as it allows the user to compare the power that they generate to that of the wind turbine. The hand crank itself was designed and constructed by the previous capstone team. The crank has an emergency brake where, if the crank is turned at a speed higher than 450 RPM, the brake is enabled to ensure that the crank's mechanical parts do not fail. The three-phase AC output of the hand crank is rectified to DC and connected to a resistive load. As the generator produces a higher current, more torque is required to turn the crank. As a result, we needed to identify an appropriate resistance value for the system.

Error! Reference source not found.

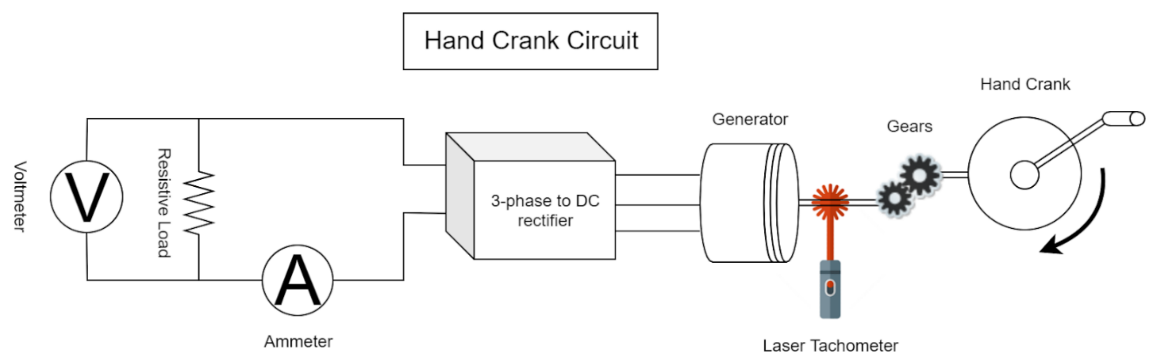

Figure 6 Hand Crank Power Circuit used to determine resistive load

Rectifier

The three-phase AC line to line output of the hand crank is converted to DC via a rectifier. We selected a store-bought rectifier that is rated for 1200V and 50A which provides plenty of overhead for our anticipated maximum voltage and current.

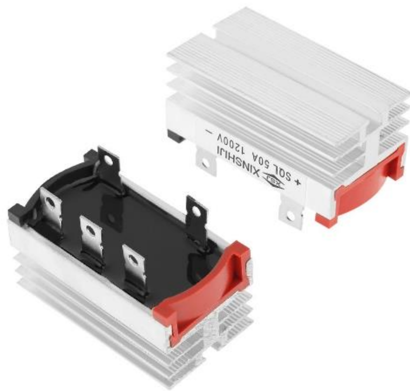

Figure 7 3-phase AC to DC rectifier

Resistors

When selecting the resistive load for the generator, there are two important factors that played a role in our design decision. We want the power generated by the hand crank to be on the same order of magnitude as the turbine, but we also wanted the hand crank to be relatively easy to turn. With that in mind, we also know that as the current produced by the generator increases, it becomes harder to turn. To determine the appropriate load, we used 6Ω resistors rated for 50W and connected them in series to find the appropriate load for the system. During our tests, a team member generated 54W of power when the crank was connected to an 18Ω load. Assuming it is possible for someone to generate a voltage that is 1.5 times higher than our teammate did, we predict the theoretical maximum power produced to be 122W, which is within the power rating of 3 50W resistors in series (150W).

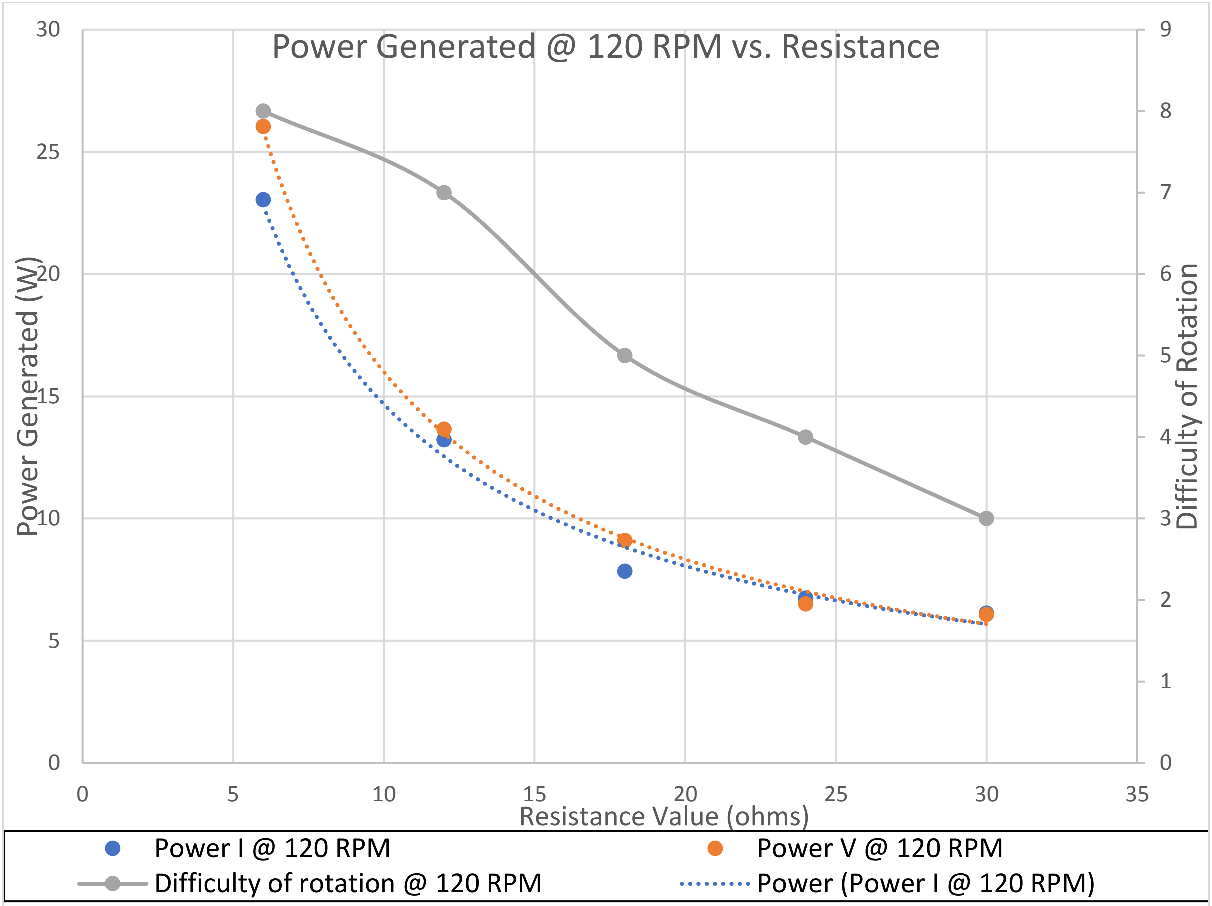

Figure 8 Power generated and Relative Difficulty of Rotation at 120RPM vs. Resistance

2.5. Environmental Sensor

Option A: BME680

The requirement to measure humidity and temperature is satisfied by the HIH6030 environmental sensor. Over the course of the design phase, two sensors were tested – the BME680 and the HIH6030. The BME 680 sensor has been selected by the previous capstone.

The BME680 sensor integrates the humidity and temperature sensor into one package. It communicates with the microcontroller via I^2C, satisfying the communication requirement in the functional specification. Additionally, the tolerance of the temperature sensor is ±0.5 °C at a nominal working temperature of 25 °C. The worst-case tolerance is ±1 °C, which matches our tolerance requirement exactly.

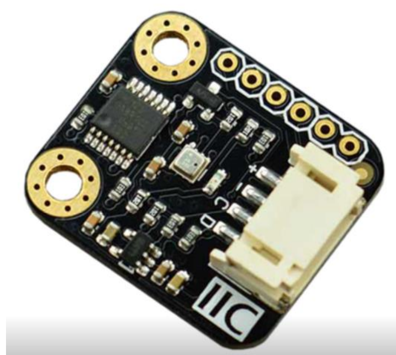

Figure 9 BME680 sensor

However, despite the sensor meeting all the requirements it proves to be the cause of issues during the integration phase of the project. This sensor has a large code footprint due to its complexity and requires 432 bytes of volatile memory to operate. Using this sensor, we run into reliability issues with the board causing failures during the initialization routine due to insufficient RAM. For primarily this reason, a different environmental sensor is chosen, which has very little code overhead.

Option B: HIH6030 IC

The HIH6030 is a temperature and humidity sensor offered in an 8-SOIC package. It is capable of temperature and relative humidity measurements of ±4.5% and ±1°C tolerances, respectively. It offers communication via I^2C and is soldered directly on the main circuit board. With a -40-100°C operating range and a low RAM requirement of 14 bytes, this is the sensor chosen for the final product.

Figure 10 HIH6030 sensor

2.6. Human Presence Sensor

A human presence sensor is required to identify when a person is standing in front of the display from requirement 4 in the design requirements. When a person is detected, the displays turn on and the user can interact with the system via the hand crank. We explored two options for this requirement – the AK9753 sensor, and the Omron D6T-1A-02 sensor.

Option A: AK9753 Sensor

The AK9753 features 4 integrated infrared sensors allowing the detection of a person standing in front of it. The position of these sensors is shown in **Error! Reference source not found.**Figure 11, taken from the AK9753 datasheet.

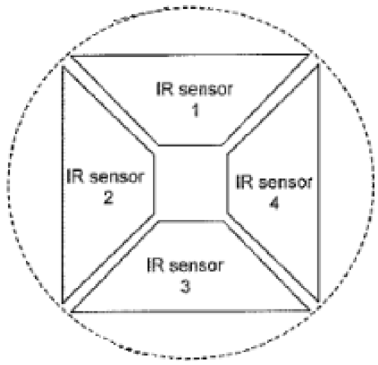

Figure 11 IR sensor configuration on the AK9753 sensor

It features an I^2C interface allowing easy communication between itself and the microcontroller. The operating temperature of -30-85°C makes it suitable for use outdoors. However, the large viewing angle of 160° and the legs of the sculpture placed 45° apart means there will likely be issues with false positive readings when the sensor detects the sculpture instead of a human.

Option B: Omron D6T-1A-02

Figure 12 D6T-1A-02 detection sensor

The Omron sensor incorporates a temperature sensor used for human presence detection. By comparing the temperature in its field of view to the ambient temperature, it can detect human presence. As with the AK9753, this sensor also features an I^2C interface. Additionally, the sensor has an operating temperature of -40-80°C, making it also suitable for outdoor use. Due to the simplicity of this sensor and the more suitable sensing technology for this application, this sensor has been selected for the project.

The sensors are summarized in Table 2.

	D6T-1A-02	AK9753
Technology	Temperature	Infrared
Communication protocol	I^2C	I^2C
Operating Temperature	-40-80°C	-30-85°C
Field of View	26.5°	160°
Selected for project	Yes	No

Table 2 Comparison of human presence detection sensors

2.7. Current Measurement

We examined two options for current measurement. The first option is to use single pass through hall effect sensor, and the second option is to use a hall effect sensor IC.

Option A: HO-series LEM Sensor

The first option for current sensing is using a single pass through hall effect sensor, shown in Figure 13. These devices do not require the current to pass through the PCB, the wire is inserted into a circular gap in the sensor. Therefore, none of the measured current is flowing through the PCB and the problems associated with high current on the PCB tracks are avoided.

Figure 13 LEM HO-P Series Hall Effect current sensor

These sensors have a maximum current rating that is selected based upon the maximum current we expect from the turbine and crank. We tested the LEM HO 25-P and LEM HO 10-P which have maximum current ratings of 25A and 10A, respectively.

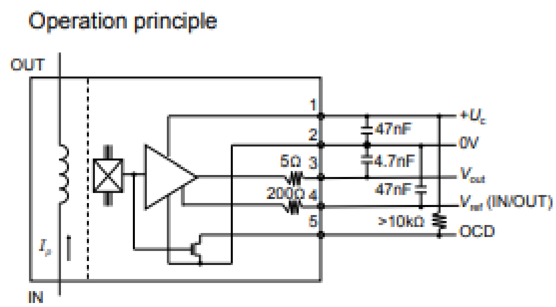

Figure 14 Simplified diagram of hall effect sensor

The output of the sensor is a simple linear function of the current passing through it.

$$V_{out} = V_{ref} + G_{th}I_pN_p = V_{ref} + G_{th}I_p$$

Where G_{th} is the theoretical sensitivity, I_p is the current to be measured, V_{ref} is the reference voltage (internally set to 2.5V) and N_p is the number of turns of the wire which is 1 in our case. G_{th} is a number ranging between 32-100 mV/A depending on the model of the sensor.

Option B: ACS723 Hall Effect IC

The second option is to have the current passing through the PCB and use a hall effect IC. This option became more viable once the requirement for current was reduced from 25 A to 5 A as a result of further wind turbine testing. For the final design, we select the ACS723 hall effect current sensing IC, shown in Figure 15.

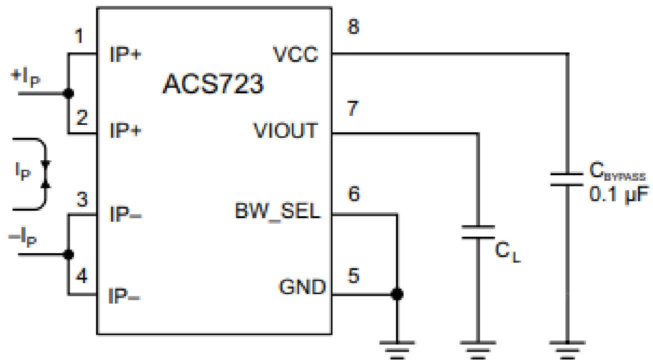

Figure 15 ACS723 current sensing IC

The main advantage of the ACS723 IC over the HO-series current sensor is the greatly increased resolution. The ACS723 IC has 4x the resolution of the HO 6-P, allowing the detection of currents as small as 12.5 mA. Additionally, the ACS723 costs only $3.27 while the HO 6-P costs $22.47.

	ACS723	HO 6-P
Maximum Current (A)	5	6
Sensitivity (mV/A)	400	100
Maximum Resolution (mA)	12.5	50
Price ($)	3.27	22.47

Table 3 Comparison of ACS723 and HO 6-P

Like the HO-series sensor, the output voltage is a linear function of the measured current.

$$V_{out} = V_{ref} + G_{th} I_p$$

Where V_{ref} = 2.5 V, G_{th} = 400 mV/A, and I_p is the current to be measured.

2.8. Voltage Measurement

The 3 voltage measurements use a voltage divider circuit consisting of 2 resistors, as shown in Figure 16 Voltage dividerFigure 16. V_{sense} is the maximum voltage the microcontroller can sense, which is 5 V. $V_{meas,max}$ is the maximum voltage we expect from the component.

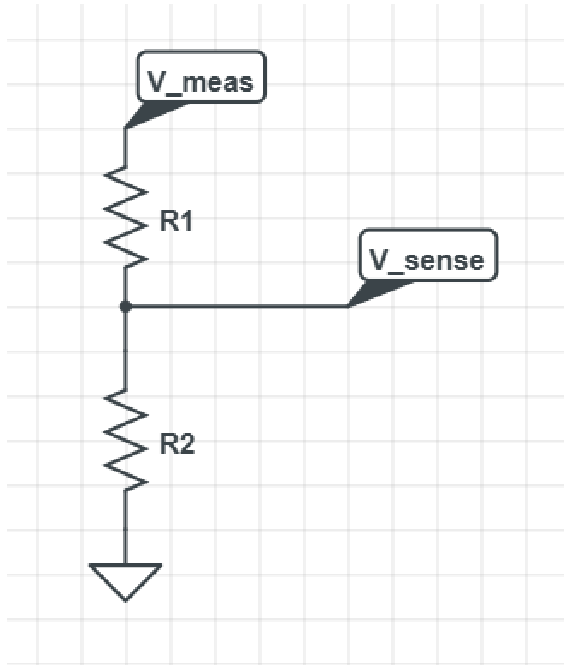

Figure 16 Voltage divider

Hand crank voltage sensing

$$\frac{V_{sense}}{V_{meas,max}} = \frac{5}{45} = \frac{R_2}{R_1 + R_2} \Rightarrow \frac{R_1}{R_2} = 0.11 \Rightarrow R_1 = 10\ k\Omega, R_2 = 91\ k\Omega$$

Wind turbine voltage sensing

$$\frac{V_{sense}}{V_{meas,max}} = \frac{5}{15} = \frac{R_2}{R_1 + R_2} \Rightarrow \frac{R_1}{R_2} = 0.33 \Rightarrow R_1 = 10\ k\Omega, R_2 = 22\ k\Omega$$

Battery Voltage sensing

$$\frac{V_{sense}}{V_{meas,max}} = \frac{5}{15} = \frac{R_2}{R_1 + R_2} \Rightarrow \frac{R_1}{R_2} = 0.33 \Rightarrow R_1 = 10\ k\Omega, R_2 = 22\ k\Omega$$

Where the deviation in the chosen resistors from the theoretical values comes from choosing from a list of standard resistance values.

2.9. Microcontroller

We considered two microcontroller families when making the choice for this project – the ATMega series and the STM8 series. As indicated in item 8 of the requirement specification, the microcontroller must:

1. Be able to communicate with sensors and displays
2. Have at least 32kB flash and 2kB volatile memory
3. Have at least 4 ADC channels of at least 10-bit resolution
4. Good online documentation and a simple IDE

The communication requirement is satisfied by an I^2C peripheral on the chosen microcontroller. Many sensors support this standard, as well as the displays discussed in section 2.10.

Our justification of having at least 2kB volatile memory was largely based on the displays we chose. Since each OLED requires a 1kB buffer, we chose to have a minimum of 2kB of memory to allow 1kB for the extra variables that will be required to run the main program. The 32kB of program memory was an estimate to safely allow us to have enough overhead to increase the firmware complexity if needed.

The need for 4 ADC channels comes from the power sensing. We require three ADC inputs for measurement of the battery, hand crank, and turbine voltage. We require one ADC input for the current sensor input. The need for a 10-bit resolution is our decision based on the precision needed for these sensors. Due to the application and sensor choice, we concluded that an ADC resolution of 5mV is adequate.

	ATMega series	STM8 series	ATMega328P
Flash Memory	4kB-128kB	16kB-128kB	32kB
SRAM	512B-4kB	2kB-6kB	2kB
ADC channels	6-8 x 10 -bit	10-16 x 10-bit	6 x 10-bit
I^2C Functionality	Yes	Yes	Yes
Price	\$2.85 – 11.00	\$3.10 – 6.50	\$3.32

Table 4 Microcontroller Comparison

Many microcontrollers satisfy these criteria, and so we emphasized the 4th criterion. Due to our prior experience and the large amount of documentation available, we choose the ATMega328P microcontroller, which works well with the Arduino IDE and satisfies the above requirements. The ATMega328P specifications of interest are summarized in Table 4.

2.10. Display Dashboard

The display board hosts the electronic displays for interaction with users. The metal front plate has been previously designed to show the information to the user and the display board hosts the electronics for driving the displays.

As discussed with the client, the initial dashboard designed by previous Capstone groups was deemed unsatisfactory for our requirements and has been redesigned for this year. The main issues with the previous design was the lack of an appropriate space for the hand crank, as well as problems with displays readability. The new design features larger displays, to enhance visual appeal and readability. It consists of 4 OLED displays that allow users to receive real-time information on the weather conditions such as temperature and humidity around the structure, as well as information of the power generated by the wind turbine and hand crank. A fifth OLED display shows the highest power generated by the hand crank since its installation. There is also a scale made of LEDs that provide an indication of the power consumption of common household electronics. The scale compares the power output of the hand crank to that of household appliances by lighting up a strip of RGB-LED lights in increasing increments. This aims to motivate users to turn the hand crank and discover how the system operates. Some final details are still pending such as text describing the purpose of the project as well as the land acknowledgements which will be provided by the client. The display board will be made from aluminum sheet metal with slots water jet cut for the displays and motion detector, however, due to concerns with COVID-19, our group was unable to find a metal shop to have the board fabricated.

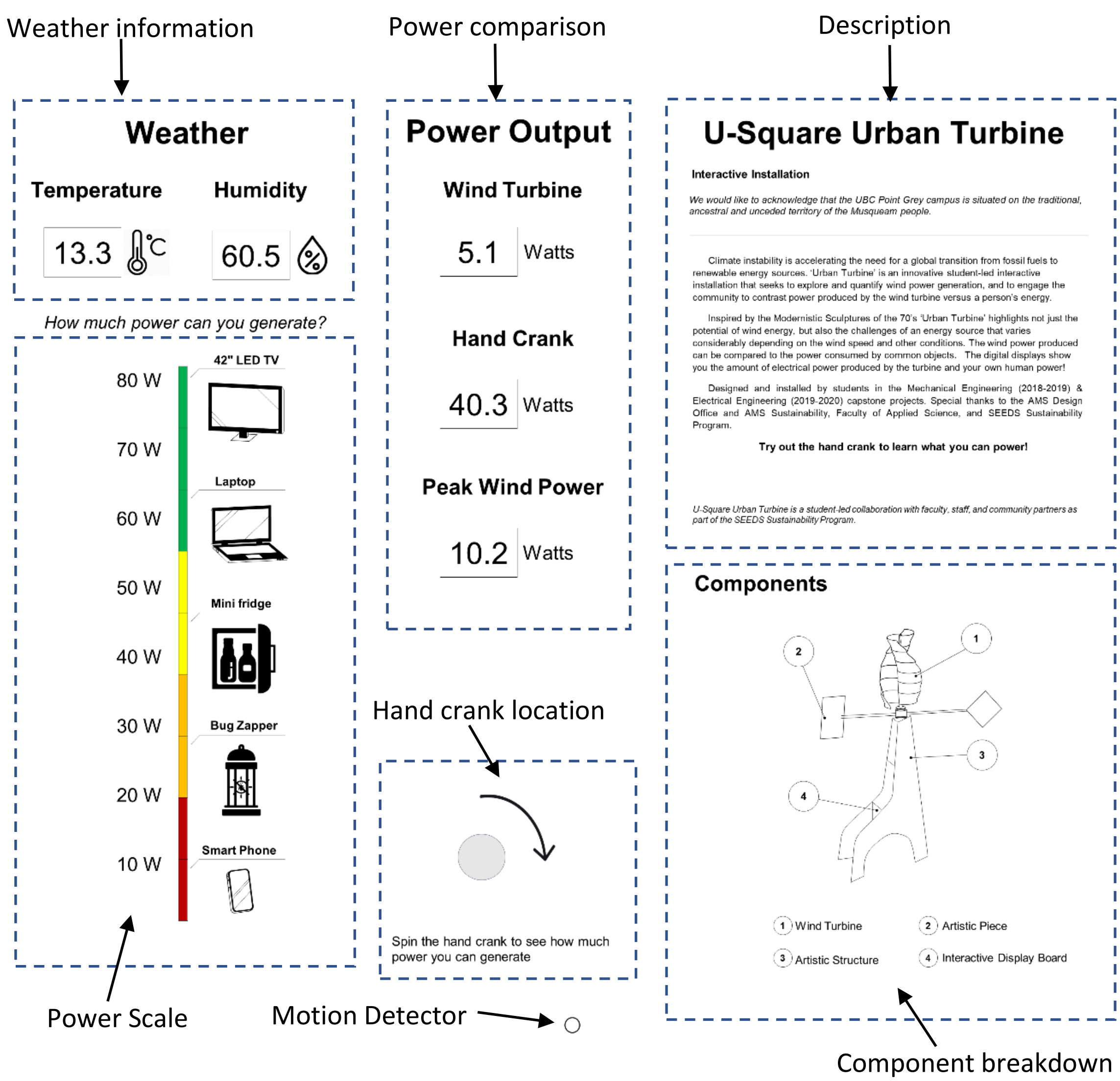

Figure 17 The dashboard design

Since the displays are a critical element of the interactive dashboard, several technologies were considered. The technologies were narrowed down to the following:

- 7-segment displays
- Liquid crystal displays (LCDs)
- Organic LEDs (OLEDS)
- E-paper displays

The main factors considered when choosing the displays are listed below:

- Readable in daytime conditions (under direct sunlight)
- Wide operating temperature to operate in winter and summer conditions
- Low power consumption (ideally under 1W)
- Display made of waterproof materials. Although it can be packaged to prevent water damage
- Suitable refresh rate for the displays that will show real-time power generation data

Readability and operating temperature are the most important factors to consider due to the location of the display board. Power consumption and refresh rate are secondary factors since other adjustments can be made such as sizing a bigger battery suited for the display’s power consumption.

We tested the following displays:

- Nokia 5110 (LCD)
- Adafruit 7-segment display
- LCD Character displays
- 3" Graphic Display 128x64 LCD
- 2.4" OLED Display Module 128x64

It was found that the 2.4” OLED display module meets all of our requirements. This display is readable in daytime conditions with wide viewing angles, and it has relatively low power consumption (<600mW). Two green OLED displays are being used to display power reading, and three white OLED displays are being used to display temperature, humidity and highest power generated by the hand crank. These displays are shown in Figure 18.

Figure 18 2.4" OLEDs selected for the project

2.11. Printed Circuit Board

The microcontroller, sensing circuits, I²C multiplexer and IO connectors for sensors and displays are all mounted on a single double layer printed circuit board.

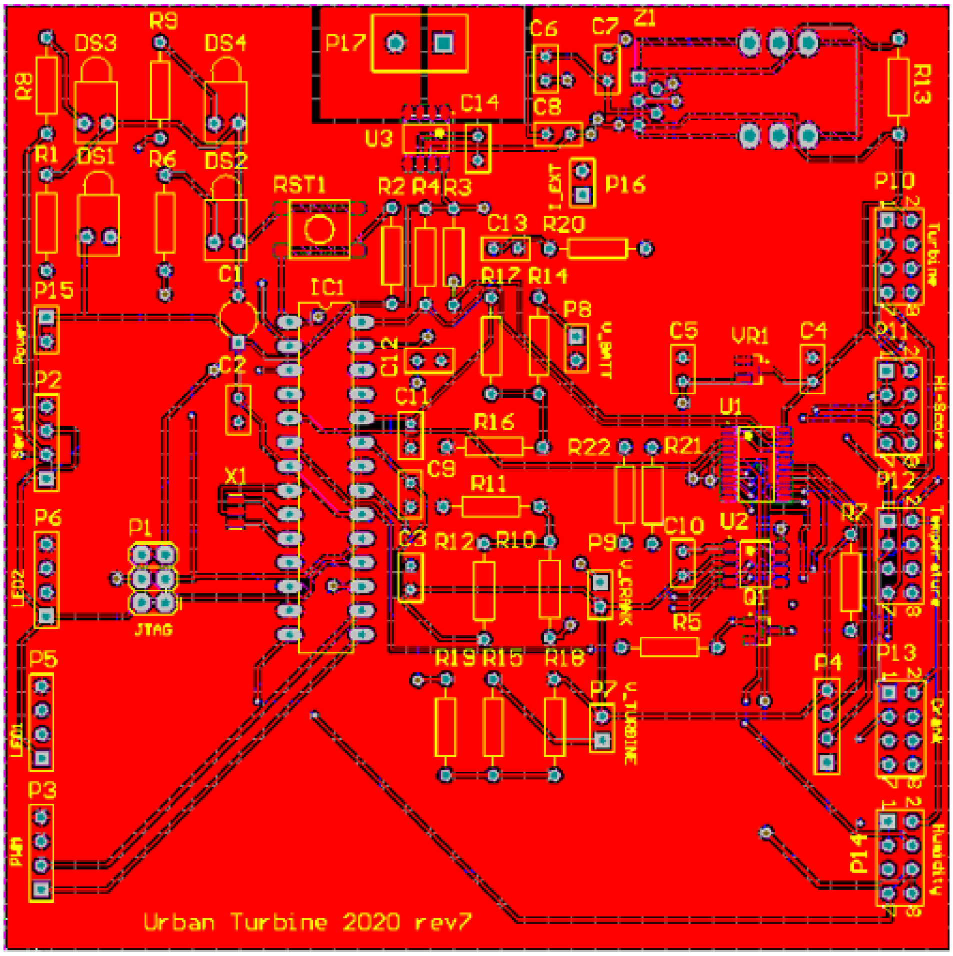

Figure 19 PCB (Top Layer View)

For PCB layout, we created planes for the turbine current input to allow for the estimated maximum turbine current of 5A.

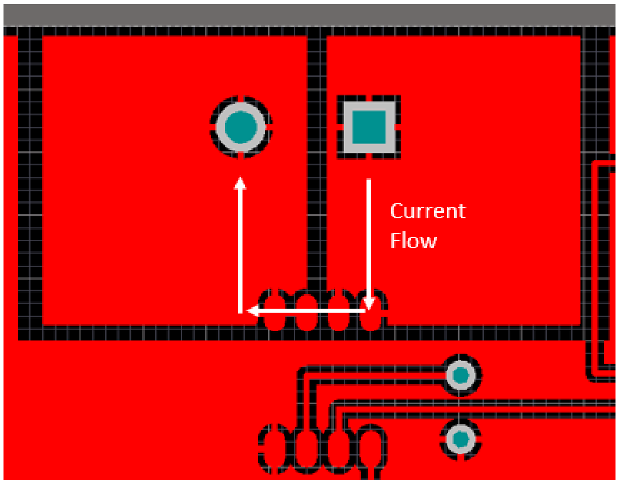

Figure 20 PCB planes for turbine current

Two common footprint options are available for the ATMega328 microcontroller - a compact surface mount package (TQFP), and a through-hole compatible package (PDIP). The compact design of the TQFP package allows the printed circuit board to be smaller, and cheaper to manufacture, however requires an additional TQFP compatible IC programmer to burn the initial Arduino bootloader onto the chip, thus making initial prototyping much harder.

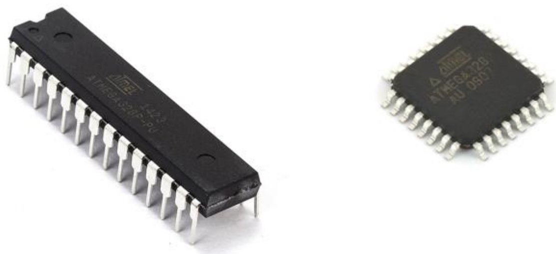

Figure 21 ATMega328 PDIP package (left) and TQFP package (right)

Furthermore, the package makes it difficult to switch out the component should it become damaged. The PDIP package is bigger, taking up more room on the PCB, however its package can be mounted on a breadboard or perfboard via a PDIP socket. This provides the ability to prototype and replace the chip if damaged. For this reason, the PDIP package was selected.

This decision also impacted the choice when selecting component form factor. Initially, SMD components were selected due to their compact size. However, as size is not a restricting factor for the design of the PCB, through-hole components are also considered, and ultimately opted for due to ease of soldering without need for a reflow soldering oven.

2.12. Firmware Design

The firmware is designed using an interrupt-driven approach, with a focus on robustness and reliability. To satisfy the human detection requirement 10.3, we configure a timer to generate interrupts at 3 Hz. This is the frequency at which the detection sensor is sampled. The timer output compare register (OCR) issues an interrupt when the timer reaches the values stored inside it. The timer restarts and the timer ISR executes. To configure the OCR, the following formula is used

$$OCR = \frac{f_{clk}}{prescaler * \ f_{int}} - 1$$

Where f_{clk} is the clock frequency of 16MHz, prescaler is the timer prescaler configured to 1024, and f_{int} is the desired interrupt frequency of 3Hz. This formula gives OCR = 5207. The human presence detection algorithm is computed during every interrupt. The detection algorithm using the Omron D6T sensor is shown in Figure 22.

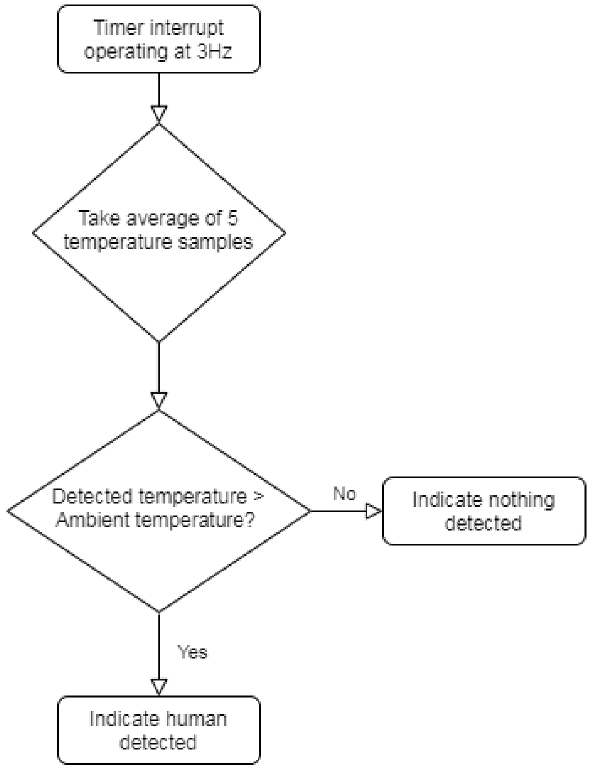

Figure 22 Human presence detection algorithm

To satisfy the robustness requirement 10.4 in the design requirements, we implement a watchdog timer to force a reset of the microcontroller in case of an unforeseen exception that leads to an infinite loop. The watchdog timeout period is set to 8 seconds, and every iteration of the main loop the timer is reset. If the watchdog timer is not reset in the specified timeout period, a watchdog timeout exception is signalled, and the system is restarted. This prevents the system from being stuck in an infinite loop.

See Appendix C for the main source code and a link to the code repository.